Ion-wake-induced anomaly of dust lattice mode in the presence of an external magnetic field

Saurav Bhattacharjee* and Nilakshi Das†
Department of Physics, Tezpur University, Tezpur, Assam, 784 028, India
(Received 9 April 2013; revised manuscript received 11 June 2013; published 29 October 2013)

We report a theoretical investigation of the dust lattice (DL) mode in two-dimensional Yukawa crystals in the presence of asymmetric ion flow and an external magnetic field perpendicular to the crystal plane. Two mutually perpendicular modes are found to be coupled due to Lorentz force. Interaction among the dust grains along the vertical direction of ion flow is strongly affected due to the formation of an ion wake. This causes anisotropy in interaction strength along two mutually perpendicular directions. Both hybrid modes are studied as characteristics of different ion flow speeds and magnetic field strengths. The study shows a fluctuation in DL mode frequency driven by the strength of the particle-wake interaction. The effect of ion flow on polarization of the hybrid wave amplitudes is discussed in detail. Results show a possible mechanism of anomalous phase transition in dusty plasma.

DOI: 10.1103/PhysRevE.88.043106 PACS number(s): 52.27.Lw, 52.30.−q

I. INTRODUCTION

The presence of micron-sized solid particles in plasma adds a new dimension to it. Because of the large and fluctuating charge on dust grains various novel and rich phenomena arise in the plasma. Highly charged dust grains of nanometer to micrometer size interact with each other through the repulsive Yukawa potential. Under the influence of a strong repulsive potential, particles may form fluid and crystalline structures. This provides an interesting phase of dusty plasma that facilitates the study of various problems of fundamental physics such as phase transition and crystal defects. Research on dusty plasma has seen an exponential growth after the discovery of plasma crystal by two pioneering groups, led by Chu *et al*. [1] and Thomas *et al*. [2] in 1994. The crystal structures include, starting from the one-dimensional (1D) [3] chain, 2D [4] and 3D cubic crystals having different lattice geometries such as triangular, fcc, bcc, and hexagonal [1]. Recent experiments under microgravity conditions provide an extended system of complex plasma for further investigation [5].

The discovery of low-frequency dust mode in plasma [6] has triggered interest in studying other waves like dust ion acoustic waves [7], electrostatic dust ion cyclotron waves [8], and dust lattice (DL) waves [9]. Melandsø [10] predicted theoretically the existence of DL waves in 1996. This mode was experimentally observed in low-temperature laboratory dusty plasma discharges by Homann *et al*. [11] in 1997. In recent years, a variety of linear and nonlinear modes of DL waves has been investigated both experimentally and theoretically [12,13]. In the presence of a magnetic field perpendicular to the crystal plane, two mutually perpendicular modes of a 2D Yukawa crystal were found to be coupled due to Lorentz force [14]. This leads to two new hybrid modes of high- and low-frequency branches instead of two independent modes.

As dust crystals are formed near the sheath region, the plasma flow dynamics near the sheath give rise to various attractive potentials such as shadowing and wake potential in addition to the repulsive Yukawa type of interaction among dust grains. Closer to the lower electrode the velocity of the ion stream towards the negatively charged electrode may lead to instabilities like fluctuation in particle positions [15,16] and develop a new kind of potential named the wake potential. This instability leaves an impact on the DL modes as well. It is identified as the possible cause for melting of dusty plasma crystals. Ivlev *et al*. [17] have reported an interesting theory on the anisotropic DL mode. They have also reported a decrease in frequency of the DL modes due to particle-wake interaction. In 2001 Joyce *et al*. [18] presented for the first time a simulation model to study the behavior of plasma crystals, incorporating both short-range Yukawa potentials and long-range wake potentials. They reported the formation of vertical strings of dust grains along the downward flow direction. Ling *et al*. [19] have experimentally demonstrated the formation of quasi-2D dusty plasma with vertical chains of dust particles aligned through the wake-field effect of downward ion flow. In recent years, there have been experimental reports on the formation of 1D vertical strings [20] and self-organized formation [21] of vertically aligned 1D vertical chains to 2D and 3D bundle structures of dust grains.

Ion-wake structures and their dynamics have been extensively studied in the absence of a magnetic field. However, very limited theoretical and experimental studies [22,23] in the presence of a magnetic field are available. In the limit of linear response theory, Nambu *et al*. [22] have reported a damping of wake strength in the presence of a magnetic field. This leads to a weak effective interaction strength between dust grains along the vertical direction compared to the unmagnetized case and has been verified experimentally [23] in recent years. In a recent paper Saurav *et al*. [24] investigate the effect of wake potential on Coulomb crystallization in the presence of a magnetic field. They observed a reduction in RDF (radial distribution function) peak heights with increased strength of the wake potential and reported an ion-wake-induced dislocation of dust grains from the regular crystal arrangement. This modification of particle-wake interactions with the strength of the ion flow in the presence of a magnetic field and its effect on various eigenmodes are important issues in complex plasma.

*sauravtsk.bhattacharjee@gmail.com
†ndas@tezu.ernet.in

The phase behavior of fluids depends solely on the intermolecular interaction. Understanding this mechanism is one of the biggest challenges in statistical thermodynamics. Ion-wake formation and its dynamics have been found to play a vital role in understanding the formation of Coulomb crystals and their phase transition in magnetized complex plasma. In this paper we presented a theoretical study to investigate the behavior of DL modes in the presence of a magnetic field perpendicular to the crystal plane and ion flow. The study shows that the effective strength of interaction along the direction of ion flow decreases with an increase in the strength of the magnetic field. This behavior is in agreement with experimental results reported by Carstensen *et al.* [23]. Polarization of both the hybrid wave amplitudes and their interplay with the magnetic field have been discussed in detail. Results show a possible kind of anomalous phase transition [25] in dusty plasma.

II. THEORETICAL FORMULATION

A. Interaction potential among dust grains

We consider a 2D uniform dusty plasma with stationary heavier dust grains in the presence of an external magnetic field $B_o\hat{x}$ perpendicular to the downstream ion flow. Under the influence of an magnetic field, the ion flow dynamics is affected and subsequently the dielectric response function [22] of the plasma medium also changes. In the presence of a low-frequency wave ($\omega \ll \omega_{ce}$),with a phase velocity lower than the electron thermal velocity, electrons will have a Boltzmann distribution. The dielectric response function can be written as [22]

$$\epsilon(\omega,k) = 1 + \frac{1}{k^2{\lambda_{\rm De}}^2} + \frac{{k_{||}}^2}{k^2}\frac{{\omega_{\rm pi}}^2}{{\omega_{\rm ci}}^2 - (\omega - k_{||}u_{\rm io})^2}, \quad (1)$$

where ${k^2} = {k_z}^2 + {k_y}^2$ and $k_z(\|)$ and $k_y(\perp)$ are wave vectors parallel and perpendicular to the direction of ion flow, respectively. In deriving Eq. (1) it was assumed that $k_\| \gg k_y$. $\omega_{\rm pi}$ and $\omega_{\rm ci}$ are the ion plasma frequency and ion cyclotron frequency, respectively, and $u_{\rm io}$ is the ion streaming velocity.

Using the electrostatic Poisson equation one can write the integral form of the interaction potential between the test dust particulate as

$$\Phi(r,t) = \frac{Q_d^2}{(2\pi)^3 2\pi\lambda_{\rm De}\epsilon_0}\int d^3k d\omega \frac{\delta(\omega - v_t k)}{k^2\epsilon(\omega,k)} e^{ik.\acute{r}}, \quad (2)$$

where all k are normalized on the scale of electron Debye length $\lambda_{\rm De}$ and $\acute{r} = r - v_t t$, v_t is the velocity of the test dust particle and Q_d is the charge of the particle. Our physical model consists of cold stationary dust grains having dust velocity $v_t = 0$ and the corresponding interaction potential takes the form

$$\Phi(y,z) = \frac{Q_d^2}{(2\pi)^3\lambda_{\rm De}\epsilon_0}\int d^3k \frac{1}{k^2\epsilon(0,k)} e^{ik.r}. \quad (3)$$

The inverse of the dielectric response function $\epsilon(0,k)$ from Eq. (1) can also be written as

$$\frac{1}{k^2\epsilon(0,k)} = \frac{1}{k^2+1} + \frac{{k_\|}^2}{(k^2+1)M^2\left({k_\|}^2 - {k_R}^2\right)\left({k_\|}^2 - {k_{\rm Im}}^2\right)}, \quad (4)$$

where $M = \frac{u_{\rm io}}{C_i}$, is the Mach number, having $c_i = \lambda_{\rm De}\omega_{\rm pi}$ as the ion acoustic wave velocity. k_R and $k_{\rm Im}$ correspond to the real and imaginary screening modes as a function of $k_\perp$, in a complex $k_\|$ plane, and are given by

$$ {k_{R,{\rm Im}}}^2 = -\frac{1}{2}\left({k_\perp}^2 + 1 - \frac{1}{fM^2} - \frac{1}{M^2}\right) \pm\sqrt{\frac{1}{4}\left({k_\perp}^2 + 1 - \frac{1}{fM^2} - \frac{1}{M^2}\right)^2 + \frac{{k_\perp}^2+1}{M^2 f}}. \quad (5)$$

Here $f = \frac{{\omega_{\rm pi}}^2}{{\omega_{\rm ci}}^2}$. In most of the experiments done on plasma crystals in the presence of a magnetic field, it is preferable to deal with a comparatively lower value of the applied magnetic field B ($f \gg 1$). In a recent experimental paper Schwabe *et al.* [26] reported observing that for a higher magnetic field $B > 2.0$ T, the plasma system becomes unstable and forms complex patterns due to filamentation of plasma particles. This puts an upper bound on the applied magnetic field strength suitable for crystal formation.

From Eq. (5), the poles k_R and $k_{\rm Im}$ are approximated in the limit of $k_\perp > \frac{1}{fM^2}$. For an arbitrary value of M, this condition is valid for $f \gg 1$, i.e., a relatively low magnetic field. In this limit, the poles become $k_R \approx \sqrt{\frac{1}{fM^2}}$ and $k_{Im} \approx \pm i\sqrt{{k_\perp}^2 + 1 - \frac{1}{M^2}}$, respectively.

Using the dispersion relation in Eq. (4) one can write the interaction potential between the test dust particulates in the presence of a magnetic field as

$$\Phi(y,z) = \frac{{Q_d}^2}{(2\pi)^3\lambda_{\rm De}\epsilon_0}\int d^3k\delta(k)\left[\frac{1}{k^2+1} + \frac{{k_\|}^2}{(k^2+1)M^2\left({k_\|}^2 - {k_R}^2\right)\left({k_\|}^2 - {k_{\rm Im}}^2\right)}\right]e^{ik.r}, \quad (6)$$

where $r = \sqrt{y^2+z^2}$. Integrating the first part on the right-hand side of the above equation gives the Yukawa potential

$$\Phi_D = \frac{{Q_d}^2}{4\pi\epsilon_0 r}\exp\left(\frac{-r}{\lambda_{\rm De}}\right). \quad (7)$$

The second part on the right-hand side of Eq. (6) is solved by performing closed contour integration for the real pole, and finally, using the saddle point integration method [29], we get the oscillatory wake potential as

$$\Phi_w(0,z) = -\frac{{Q_d}^2}{4\pi\lambda_{\rm De}\epsilon_0}2\pi\frac{\sqrt{1/f}M\sin\left(\frac{\sqrt{1/f}z}{M}\right)}{\left(\frac{1}{f}+M^2\right)\left(\frac{1}{f}-1+M^2\right)}. \quad (8)$$

B. Dispersion relation of the dust lattice wave

We have considered the simplified model of a monolayer hexagonal lattice in the Y-Z plane with ion flow along the downward vertical z direction and a magnetic field perpendicular to the crystal plane. The lattice mode propagates along the

Y direction parallel to the fundamental lattice vector directed from the center of the cell to one of its nearest neighbors. The equations of motion along two transverse directions are given by [14]

$$m_d \frac{d^2 y_{n1}}{dt^2} = \sum_{m=1,m\neq n}^{N} K_{y_{nm}}(y_{n1} - y_{m1}) + Q_d B_o \frac{dz_{n1}}{dt}, \quad (9)$$

$$m_d \frac{d^2 z_{n1}}{dt^2} = \sum_{m=1,n\neq m}^{N} \left[K_{z_{nm}} + K_{zw_{nm}}\right](z_{n1} - z_{m1}) - Q_d B_o \frac{dy_{n1}}{dt}, \quad (10)$$

where n represents the particle number in the lattice and m represents all other neighboring interacting particles. $y_{(n,m)1}$ and $z_{(n,m)1}$ are the displacement of the particles from their equilibrium positions. $K_{(y,z)_{nm}}$ are the spring constants corresponding to the Yukawa type of interaction along the y and z direction and $K_{zw_{nm}}$ is the spring constant corresponding to the wake potential along the vertical z direction.

Using Eq. (7) we can write the normalized spring constants $K_{y,z}$ corresponding to the Yukawa potential along the y and z direction as

$$K_{y,z} = \left.\frac{d^2\Phi_D}{d(y,z)^2}\right|_{y,z=a} = \frac{\Gamma \exp(-\sqrt{2}\kappa)}{2^{5/2}\kappa^2}[3 + 3\sqrt{2}\kappa + 2\kappa^2]. \quad (11)$$

Here a is the average interparticle distance, Γ is the Coulomb coupling parameter, and $\kappa = \frac{a}{\lambda_{De}}$ stands for the screening constant.

Similarly, from Eq. (8) we get the spring constant for the wake potential as

$$K_{zw} = 2\pi \frac{(1/f)^{3/2} \sin\left(\frac{\sqrt{1/f}\kappa}{M}\right)}{M\left(\frac{1}{f} + M^2\right)\left(\frac{1}{f} + M^2 - 1\right)}. \quad (12)$$

This leads to the effective spring constant along the z direction as

$$K_z = K_z(\text{Yukawa}) + K_{zw}(\text{wake}). \quad (13)$$

As we have considered that the DL mode propagates along the y direction, the oscillations of the wave modes are $y_{n1} = A_y \exp[i(k_y a - \omega t)]$ and $z_{n1} = A_z \exp[i(k_y a - \omega t)]$, respectively, along two mutually perpendicular directions. Substituting y_{n1} and z_{n1} in Eqs. (9) and (10) we get the dispersion relation as

$$\left[\omega^2 + \sum_{m=1,n\neq m}^{N} K_{y_{nm}}(\exp[ik_y a] - 1)\right]\left[\omega^2 + \sum_{m=1,n\neq m}^{N} \left(K_{z_{nm}} + K_{zw_m}\right)(\exp[ik_y a] - 1)\right] - {\omega_c}^2\omega^2 = 0. \quad (14)$$

Due to the Lorentz force, the term ${\omega_c}^2\omega^2$ appears in Eq. (14) and hence two mutually perpendicular longitudinal and transverse modes become coupled in the presence of an external magnetic field. The mixing of the modes leads to the appearance of two new hybrid modes instead of independent longitudinal and transverse modes of DL waves [6].

In the limit of $k_y a \ll 1$, Eq. (14) can be simplified to give two roots in high- and low-frequency branches as

$$\omega_H^2 \approx \omega_c^2 + \sum_{m=1,n\neq m}^{N} 2\left(K_{y_{nm}} + K_{z_{nm}} + K_{zw_m}\right)\sin^2\left(\frac{k_y a}{2}\right) \quad \text{[upper hybrid]}, \quad (15)$$

$$\omega_L^2 \approx \frac{\sum_{m=1,n\neq m}^{N}\left[2K_{y_{nm}}\sin^2\left(\frac{k_y a}{2}\right)\right]\sum_{m=1,n\neq m}^{N}\left[2\left(K_{z_{nm}} + K_{zw_m}\right)\sin^2\left(\frac{k_y a}{2}\right)\right]}{\omega_c^2} \quad \text{[lower hybrid]}. \quad (16)$$

Here, the frequency is normalized by $\omega_N = \sqrt{\frac{K_B T_d}{m_d \lambda_{De}^2}}$, where K_B, T_d, m_d, and λ_{De} are the Boltzmann constant, dust temperature, dust mass, and electron Debye length, respectively. In the limit of dust cyclotron frequency $\omega_c > 1$, Eq. (15) gives the hybrid frequency $\omega > \omega_c$ and is called the upper hybrid mode ω_H and Eq. (16) shows the hybrid frequency $\omega < \omega_c$ and is called the lower hybrid mode ω_L.

Substituting the displacements y_{nm} and z_{nm} in Eqs. (9) and (10) we can get the wave amplitude ratio along the y and z directions as

$$\frac{y_{nm}}{z_{nm}} = i\mu, \quad \text{where} \quad |\mu| = \sqrt{\frac{\omega^2 + 2(K_z + K_{zw})(\cos(k_y a) - 1)}{\omega^2 + 2K_y(\cos(k_y a) - 1)}}. \quad (17)$$

Using Eq. (14) one can write the polarization P of the wave amplitudes as

$$P = \frac{1}{1 + \frac{1}{|\mu|}}. \quad (18)$$

$P = 1$ corresponds to the pure longitudinal mode and $P = 0$ corresponds to the pure transverse mode.

III. RESULTS AND DISCUSSION

The Debye cloud surrounding dust particles gets distorted by the downward ion flow and becomes elongated along the lower vertical (z) direction. The amount of distortion and the scale length of elongation depend mainly on the strength of the magnetic field and flow velocity of the downward ion stream towards the plasma sheath. The excess positive ions

that are accumulated on the lower side of the Debye cloud attract the dust particles just below it to align along the vertical ion flow direction [15,16]. This process of alignment depends vitally on the frequency of the wake potential. It is observed from Eq. (8) that the frequency of the wake potential increases with a decrease in Mach number for a given magnetic field strength and is shown in Fig. 1(a). As the particle-wake interaction is caused by the resonance interplay between dust particles and the ion acoustic wave, dust grains are trapped or confined at the trail of the ion wake. However, this trapping is effective only for a particular range

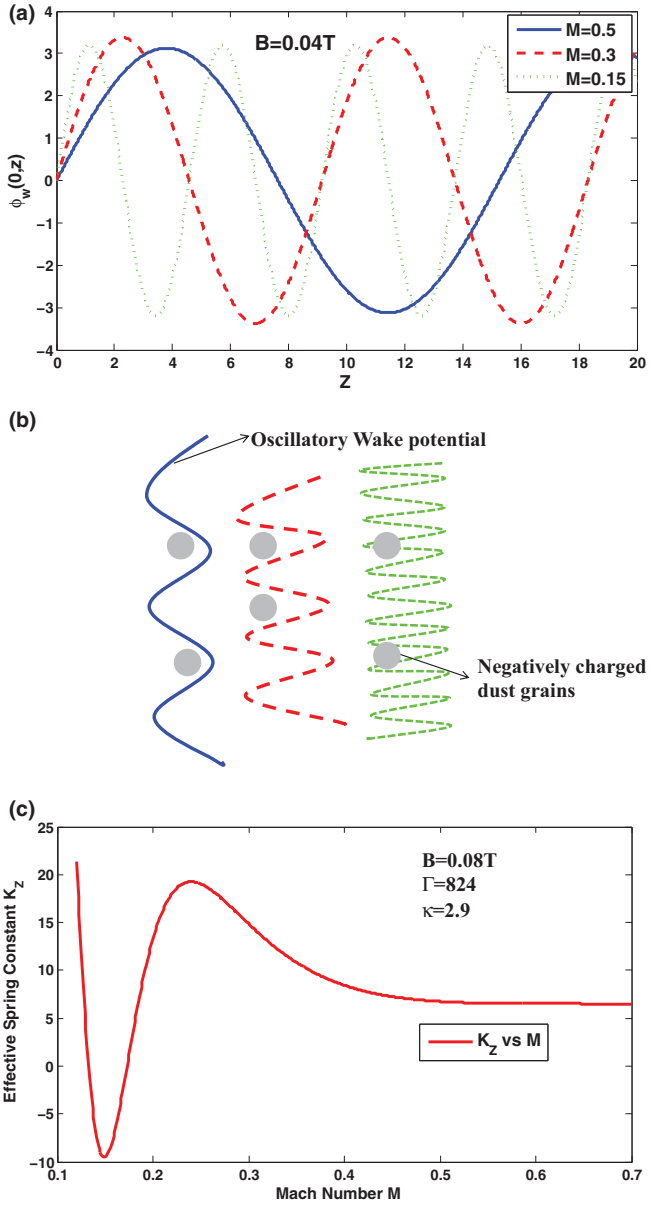

FIG. 1. (Color online) (a) Normalized wake potential for Mach number $M = 0.5$ [solid (blue) line], $M = 0.3$ [dashed (red) line], and $M = 0.15$ [dotted (green line)], having magnetic field $B = 0.04$ T. (b) Vertical confinement mechanism of particle-wake interaction with an increase in strength of the wake potential, from left to right. (c) Effective spring constant K_z vs M (Mach number) for the given set of plasma parameters.

of Mach number. For relatively longer wavelengths (higher M value) of the wake potential, the separation between the dust grains is not of the order of the trapping wave length. As a result, the resonance fails to occur and the particle-wake interaction is weak there. As we decrease the ion flow speed, for a particular range of Mach number, resonance starts taking place and the effective confinement of dust grains is dominant over that range. On a further decrease in the ion flow speed, the confinement frequency is too high to keep the resonance intact and dust particles can no longer be trapped. The whole mechanism is demonstrated in Fig. 1(b). Figure 1(c) clearly shows the transition of the effective vertical strength of interaction from Eq. (13), driven by the ion flow speed. It is evident from Fig. 1(c) that the vertical spring constant K_z undergoes a transition from a positive to a negative value and again attains a positive value, with a gradual decrease in ion flow speed for a given magnetic field strength. During positive halves of the vertical spring constant K_z, the effective interaction is repulsive in nature and during negative cycles it is attractive. We have chosen the set of plasma parameters as the number of electrons on the dust surface $Z_d = 1.5 \times 10^3$, ion plasma frequency $\omega_{\rm pi} = 1.86 \times 10^7$ Hz, dust mass $m_d = 10^{-20}$ kg, and density $n_d = 2.44 \times 10^{10}$ m^{-3}. The corresponding Coulomb coupling parameter Γ is found to be 824 and the screening strength κ is 2.9.

This interaction between dust particles and ion wake has a strong impact on the DL modes. Using Eqs. (15) and (16), it is shown in Figs. 2(a) and 2(b) that, with a decrease in ion flow speed for a given magnetic field, the Mach number at which effective interaction along the vertical ion flow direction is attractive in nature, the frequency of the DL mode is found to decrease. In this range of effective attractive interaction, the dust grains dislocate from their regular oriented position along the vertical direction and this leads to a decrease in the DL mode. On a further decrease in Mach number from which the interaction attains a repulsive nature, the dust grains get back to their original configuration and the DL mode frequency increases once again and is shown for two values of magnetic field and a given set of parameters. It is also shown in Figs. 2(a) and 2(b) that the upper hybrid cutoff frequency ω_c increases with an increase in strength of the magnetic field, in two cases.

Equations (17) and (18) show that polarization of the hybrid wave amplitudes varies with the ion flow speed as well as the magnetic field strength. The variation of polarization with ion flow speed and for a given set of parameters is shown in Fig. 3(b). The entire range of observations has been classified into three regions, depending on the behavior of polarization.

Region I ($M > 0.4$): At a comparatively high ion flow speed ($M > 0.4$), the strength of the interaction remains almost unaffected with a decrease in ion flow speed and hence increase in wake potential as shown in Fig. 1(c). In this region the polarization of hybrid wave amplitudes remains unaffected and the upper hybrid is more longitudinal in nature and the lower hybrid is more transverse in nature. On closely approaching $M = 0.4$, the polarization starts shifting and becomes equal for the two modes at $M = 0.4$, as shown in Fig. 3(b).

Region II ($M = 0.4$ to 0.24): As we decrease the Mach number below $M = 0.4$, it is shown in Fig. 1(c) that the effective spring constant, which is repulsive in nature in that region, increases and reaches a maximum at $M = 0.24$. The

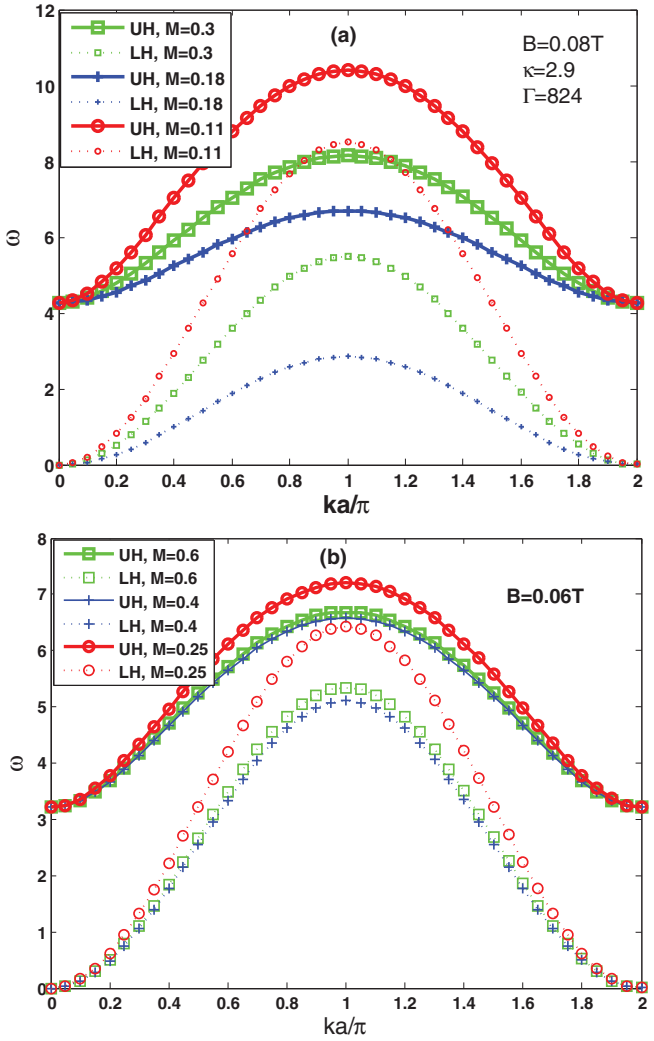

FIG. 2. (Color online) Dispersion relation profiles with different Mach numbers M and magnetic field strengths B for a Coulomb coupling parameter $\Gamma = 824$ and screening strength $\kappa = 2.9$. (a) Normalized frequency dependence of both the upper hybrid (UH; solid line) and the lower hybrid (dotted line) waves at $M = 0.3$ [(green) squares], $M = 0.18$ [(blue) crosses], and $M = 0.11$ [(red) circles], for a given magnetic field $B = 0.08$ T and upper hybrid cutoff $\omega_c = 4.27$. (b) $M = 0.6$ [(green) squares], $M = 0.4$ [(blue) crosses], and $M = 0.25$ [(red) circles] with $B = 0.06$ T and cutoff $\omega_c = 3.21$.

corresponding DL mode shows an enhancement in frequency and is shown in Fig. 3(a). In this range of repulsive zones of interaction the polarizations of both upper and lower hybrid waves become interchanged. Polarization of the upper hybrid is found to be more transverse in nature compared to the lower hybrid and it reaches a maximum at $M = 0.24$.

Region III ($M = 0.24$ to 0.17): With a further decrease in Mach number below $M = 0.24$, Fig. 1(c) shows that the effective spring constant decreases towards a negative value. The type of interaction starts to become attractive in nature. The frequency of the corresponding DL mode decreases as is evident in Fig. 3(a). In this region the polarizations of both upper hybrid and lower hybrid again are interchanged and reach a maximum value at $M = 0.17$.

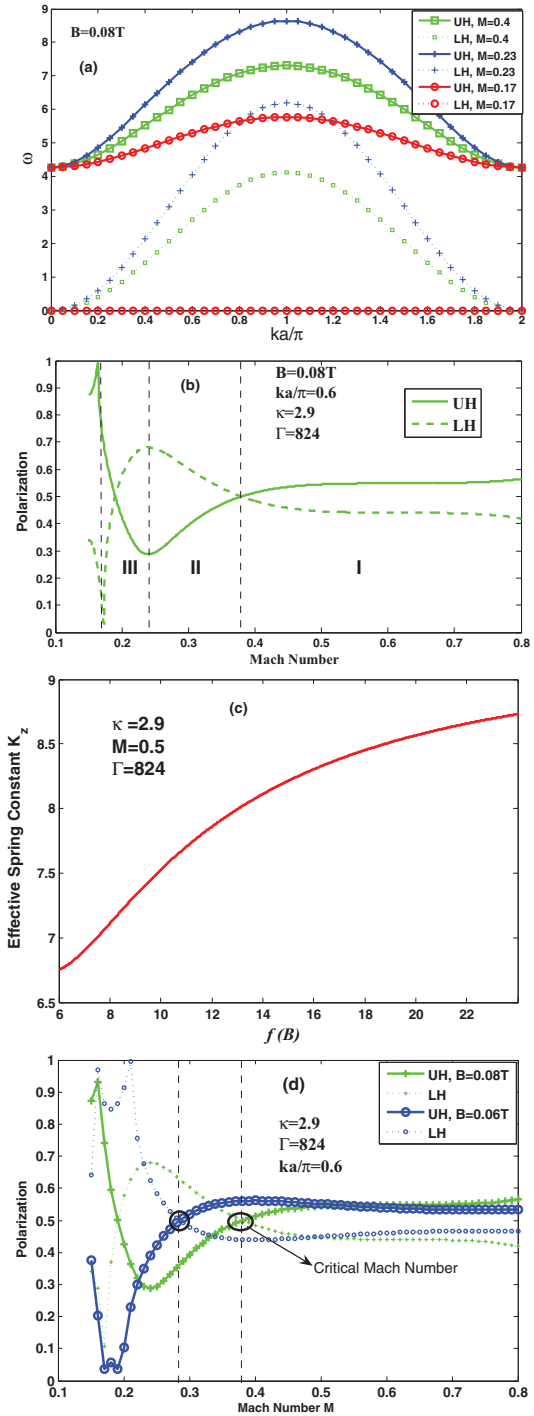

FIG. 3. (Color online) (a) Normalized frequency dependence of both the upper hybrid (UH; solid line) and the lower hybrid (LH; dotted line) waves at $M = 0.4$ [(green) squares], $M = 0.23$ [((blue) crosses], and $M = 0.17$ [(red) circles], for a given magnetic field $B = 0.08$ T. (b) Polarization P vs Mach number M, for both the UH [solid (green) line] and lower hybrid (LH) (green dotted) waves for a given wave number $ka/\pi = 0.6$ and magnetic field strength $B = 0.08$ T. (c) Strength of the spring constant k_z vs $f(B) = \omega_{pi}{}^2/\omega_{ci}{}^2$ for the given set of plasma parameters. (d) P vs M for a given wave number $ka/\pi = 0.6$ and different magnetic fields: $B = 0.08$ T [UH, (green) crosses with solid line; LH, (green) crosses with dotted line] and $B = 0.06$ T [UH, (blue) circles with solid line; LH, (blue) circles with dotted line].

It is shown in Fig. 3(c) that the effective spring constant along the vertical direction decreases with an increase in strength of the magnetic field (decrease in f value) and agrees with the experimental result [23]. This causes shifting of the critical Mach number, from which the polarization gets interchanged, to a lower value, with a decrease in strength of the magnetic field as shown in Fig. 3(d). This ion-flow-induced wake potential causes a periodic transition in the crystal phase from an ordered to a disordered state and, again, back to an ordered state. The disordered crystalline state refers to the dislocation of the particles from their regular oriented positions and change in crystal phase which is often encountered in experiments [27] and simulations [24] through a reduction in the peak height of the pair correlation or radial distribution function. This shows an analogy with the anomalous phase transitions in complex fluids and solid-state physics [28].

The interaction mechanism among dust grains is the key to understanding the dynamics of a system and its phase behavior. This also helps to reduce the multicomponent scenario of the plasma system to the one-component plasma model. The interaction potential thus obtained is governed by the dynamics of the background plasma. The crystal geometry has hardly any effect on this. Although the present analysis was carried out for a vertical 2D system, the findings of our work are equally compatible for a more general 3D (crystals and clusters) scenario involving the asymmetry arising along mutually perpendicular directions due to ion wake formation. It has been demonstrated above that the variation of the effective spring constant with the magnetic field agrees with the experimental results obtained for vertically placed dust subsystems. This clearly reflects the general compatibility of the present analysis.

IV. CONCLUSIONS

In the present work we have discussed in detail the effect of the wake potential on DL modes in terms of ion flow speed and external magnetic field for a 2D crystal structure. The observations can be summarized as follows.

(a) The ion flow near the sheath region gives rise to an attractive wake potential along the vertical direction and this causes anisotropy in the interaction strength along two mutually perpendicular directions.

(b) It is demonstrated in Fig. 1 that with a decrease in ion flow speed, i.e., an increase in strength of the wake potential, and for a given set of plasma parameters, the interaction among dust grains shows a transition from repulsive to attractive and, again, back to repulsive type. This causes a change in the arrangement of dust grains in the crystal from an ordered to a disordered to an ordered state. The impact of this mechanism on DL modes is clear from the dispersion relations plotted in Fig. 2.

(c) The polarization of both hybrid waves is also affected by the strength of the wake potential. At higher ion flow speeds, the wake potential is too weak to affect the polarization of dust grains and is visible in region I in Fig. 3(b). With a decrease in ion flow speed in region II, where the effective interaction along the vertical direction is repulsive in nature, the upper hybrid mode is found to be more transversely polarized compared to the lower hybrid for a given magnetic field and wave number. On a further decrease in M value, in region III, the interaction attains an attractive nature, the polarization of both the hybrid wave amplitudes reverses in character, and the upper hybrid mode becomes more longitudinally polarized compared to the lower hybrid. This is shown in Fig. 3(b).

(d) With an increase in strength of the magnetic field, the effective spring constant along z decreases; this agrees with the experimental result recently reported by Carstensen *et al*. [22] and is shown in Fig. 3(c). This leads the critical Mach number to shift to a lower value with a decrease in strength of the magnetic field for a given wave number. This is shown in Fig. 3(d).

(e) Finally, we conclude that particle-wake interaction is responsible for the anomalous transition in frequency of DL modes as a characteristic of the ion-flow-induced oscillation frequency of the wake potential along the vertical direction. This also implies an ion-wake-induced anomalous phase transition of the dust crystal from an ordered to a disordered to an ordered state. The mechanism is expected to play a significant role in affecting the transport properties such as the free energy, excess pressure, and diffusion coefficient of strongly coupled systems in the presence of a magnetic field.

ACKNOWLEDGMENTS

The authors gratefully acknowledge the anonymous referees for their valuable suggestions that really helped to bring the manuscript in its present refined form. We also like to thank Prof. Lin I, Department of Physics, NCU, Taiwan, for some useful discussions. Moreover, the financial support from University Grants Commission (UGC), New Delhi-110002, India, through major research project (42-795/2013 (SR)) is acknowledged.

[1] J. H. Chu and L. I, Phys. Rev. Lett. **72**, 4009 (1994).
[2] H. Thomas, G. E. Morfill, V. Demmel, J. Goree, B. Feuerbacher, and D. Möhlmann, Phys. Rev. Lett. **73**, 652 (1994).
[3] B. Liu and J. Goree, Phys. Rev. E **71**, 046410 (2005).
[4] J. B. Pieper, J. Goree, and R. A. Quinn, J. Vac. Sci. Technol. A **14**, 519 (1996).
[5] V. E. Fortov and G. E. Morfill, Plasma Phys. Control. Fusion **54**, 124040 (2012).
[6] N. N. Rao, P. K. Shukla, and M. Y. Yu, Planet. Space Sci. **38**, 543 (1990).
[7] P. K. Shukla and V. P. Silin, Phys. Scripta **45**, 508 (1992).
[8] R. L. Merlino, A. Barkan, C. Thompson, and N. D'Angelo, Phys. Plasmas **5**, 1607 (1998).
[9] X. Wang, A. Bhattacharjee, and S. Hu, Phys. Rev. Lett. **86**, 2569 (2001).

[10] F. Melandsø, Phys. Plasmas **3**, 3890 (1996).
[11] A. Homann, A. Melzer, S. Peters, and A. Piel, Phys. Rev. E **56**, 7138 (1997).
[12] S. Nunomura, D. Samsonov, and J. Goree, Phys. Rev. Lett. **84**, 5141 (2000).
[13] T. Misawa, N. Ohno, K. Asano, M. Sawai, S. Takamura, and P. K. Kaw, Phys. Rev. Lett. **86**, 1219 (2001).
[14] G. Uchida, U. Konopka, and G. Morfill, Phys. Rev. Lett. **93**, 155002 (2004).
[15] A. Melzer, V. S. Schweigert, and A. Piel, Phys. Scripta **61**, 494 (2000).
[16] V. Steinberg, R. Sutterlin, A. V. Ivlev, and G. Morfill, Phys. Rev. Lett. **86**, 4540 (2001).
[17] A. V. Ivlev and G. Morfill, Phys. Rev. E **63**, 016409 (2000).
[18] G. Joyce, M. Lampe, and G. Ganguli, IEEE Trans. Plasma Sci. **29**, 238 (2001).
[19] C.-L. Chan, C.-W. Io, and L. I, Contrib. Plasma Phys. **49**, 215 (2009).
[20] J. Kong, T. W. Hyde, L. Matthews, K. Qiao, Z. Zhang, and A. Douglass, Phys. Rev. E **84**, 016411 (2011).
[21] T. W. Hyde, J. Kong, and L. S. Matthews, Phys. Rev. E **87**, 053106 (2013).
[22] M. Nambu, M. Salimullah, and R. Bingham, Phys. Rev. E **63**, 056403 (2001).
[23] J. Carstensen, F. Greiner, and A. Piel, Phys. Rev. Lett. **109**, 135001 (2012).
[24] S. Bhattacharjee and N. Das, Phys. Plasmas **19**, 103707 (2012).
[25] A. B. de Oliveira, E. B. Neves, C. Gavazzoni, J. Z. Paukowski, P. A. Netz, and M. C. Barbosa, J. Chem. Phys. **132**, 164505 (2010).
[26] M. Schwabe, U. Konopka, P. Bandyopadhyay, and G. E. Morfill, Phys. Rev. Lett. **106**, 215004 (2011).
[27] R. A. Quinn and J. Goree, Phys. Rev. E **64**, 051404 (2001).
[28] T. Nagase, A. Nino, T. Hosokawa, and Y. Umakoshi, Mater. Trans. **48**, 1651 (2007).
[29] P. M. Bellan, *Fundamentals of Plasma Physics* (Cambridge University Press, Cambridge, UK, 2006).